Control-Based Design of Free-Piston Stirling Engines

José A. Riofrio, Khalid Al-Dakkan, Mark E. Hofacker, and Eric J. Barth

Abstract − **A control-based analysis and characterization of a free-piston Stirling engine is presented, and proposed as a lightweight power supply for untethered robots. Typically, such devices are designed from the point of view of a thermodynamic cycle in terms of traditional thermodynamic equations of state. Such equations of state are independent of time and therefore lend little insight when dynamic elements are incorporated into the design. The approach presented here is from a system dynamics and control perspective. Equations of state are replaced by dynamic system modeling elements. Utilizing these dynamic elements, control concepts are applied to evaluate a given configuration and ensure an unstable oscillatory response and therefore transform heat into useful work. A simulation of a commercially available free-piston engine is presented, and standard control design tools are applied to its linearized model. The results show promising potential in utilizing small-scale free-piston Stirling engines as portable power supply for robotic systems.**

Nomenclature

A	displacer area
A_r	displacer rod area
b	damping coefficient between displacer rod and piston
b_d	damping coefficient between displacer and wall
b_p	damping coefficient between piston and wall
g	acceleration of gravity
k_d	spring constant for displacer
k_p	spring constant for piston
l_d	equilibrium length of displacer spring
l_p	equilibrium length of piston spring
m_d	mass of displacer
m_p	mass of piston
P	pressure in working gas
P_{atm}	atmospheric pressure
P_0	initial pressure in working gas
T_h	temperature in hot side
T_k	temperature in cold side
V_h	volume in hot side
V_{h0}	initial volume in hot side
V_k	volume in cold side
V_{k0}	initial volume in cold side
V_r	volume in regenerator
x	displacer position
$\dot{x}$	displacer velocity
$\ddot{x}$	displacer acceleration
y	piston position
$\dot{y}$	piston velocity
$\ddot{y}$	piston acceleration

I. Introduction

The need for an effective portable power supply for human-scale robots has increasingly become a matter of interest in robotics research. Current prototypes of humanoid robots, such as the Honda P3, Honda ASIMO and the Sony QRIO, show significant limitations in the duration of their power sources in between charges (the operation time of the humanoid-size Honda P3, for instance, is only 25 minutes). This limitation becomes a strong motivation for the development and implementation of a more energy dense source of power. Put simply, state-of-the-art batteries are too heavy for the amount of energy they store, and electric motors are too heavy for the mechanical power they can deliver, in order to present a combined power supply and actuation system that can deliver human-scale mechanical work in a human-scale self contained robot package. The motivation details are discussed more thoroughly in [1].

Stirling engines are typically regarded for their high efficiency, since they are theoretically capable of achieving the Carnot thermodynamic efficiency given by $(T_{hot} - T_{cold})/T_{hot}$. Despite this fact, Stirling engines have found few applications mainly due to the low power density of current engine designs. This is in part due to the relatively large piston and displacer masses, and thus low operational frequency of the engine. Reduction of piston and displacer masses to increase the frequency and thus power output of an engine often results in recognized scaling problems where friction and leakage dominate and lead to a non-functioning engine. One potential solution to this problem of scaling is to replace traditional pistons involving frictional seals with an alternative such as elastic diaphragms. To bring about such a change, new design tools are needed to understand, or even exploit, the combined stiffness and inertia effects such an element would have on the operation of a free piston Stirling engine.
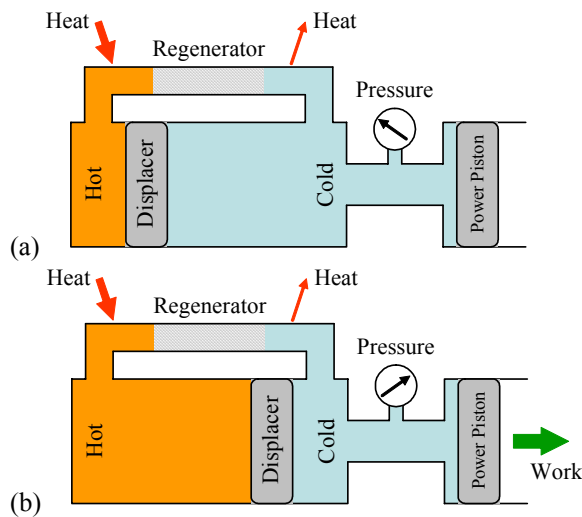
Figure 1: Schematic diagram of the displacer piston. Movement of the displacer shuttles compressible fluid between hot and cold sides of the engine with a resulting change in pressure. The regenerator stores and retrieves heat energy. With negligible flow restriction through the regenerator, there are no pressure forces on the displacer.

A brief primer on Stirling engines, and their free-piston variant, is in order. The basic operational principle of a Stirling engine comes down to the displacer chamber. As shown in Figure 1, the displacer chamber is subjected to a heat source on one end (heater), and a heat sink on the opposite end (cooler). The movement of the displacer shuttles compressible fluid between the hot space and the cold space. For example, as the displacer moves to the right, it moves gas from the cold side to the hot side where it absorbs heat resulting in an increase in gas temperature and pressure. As the displacer is moved in the opposite direction, the gas temperature is decreased thus decreasing the pressure. It is important to note that because of the flow-path connection between the two sides, there is no pressure difference across the displacer and therefore no pressure induced forces on the displacer. Without appreciable sliding friction or flow restrictions, it takes only the work required to move the displacer's inertia to change the pressure. If the displacer is additionally connected to a conservative forcing source, such as a spring, it theoretically takes no net work to vary the pressure.

Ultimately, useful work is extracted from the varying pressure of the displacer chamber by linking the cold side (usually) to a power piston chamber. Stirling engines typically utilize a regenerator to increase their efficiency. The regenerator section is packed with a material of high thermal conductivity (additionally promoted with a high surface area), high thermal capacitance, and presenting little flow restriction – usually a "steel wool" or metal screen material. The job of the regenerator is to remove and store heat energy from the gas as it moves through the regenerator section from the hot side to the cold side, and consequently return this heat energy to the gas as it moves back into the hot side. This energy storage mechanism allows the temperature of the gas to vary without rejecting as much

heat energy to the outside environment, and hence improves the thermal efficiency of the engine.

Not shown in Figure 1 is how the power piston, or simply "piston", is linked to the displacer. As previously noted, no forces (or small forces) are imposed on the displacer. For the displacer to move, and hence vary the pressure forces on the piston in order to extract work from the engine, the displacer must be linked, either kinematically or dynamically, to the motion of the piston. Free-piston Stirling engines provide a dynamic as opposed to kinematic link.

While Stirling engines have been studied exhaustively in the past, the predominant approaches to their design have been based on thermo-fluidic analysis tools, such as the Carnot theorem and the second law of thermodynamics. Additionally, the implementation of free-piston Stirling engines has been mostly limited to standard piston / cylinder devices, which typically have to provide adequate sealing between the piston and the displacer rod, and between the piston and the cylinder wall. Figure 2 shows a photo and schematic of the Sunpower B-10B free-piston Stirling engine demonstrator, developed by Sunpower Inc. This device weighs just under a kilogram and produces a nominal power of 1 Watt. A simple thermodynamic analysis of this type of device is offered in [2], and relies mostly on equations of state and intuitive notions of gas dynamics. This engine configuration was invented by William Beale in the 1970s and set the standard for future devices.
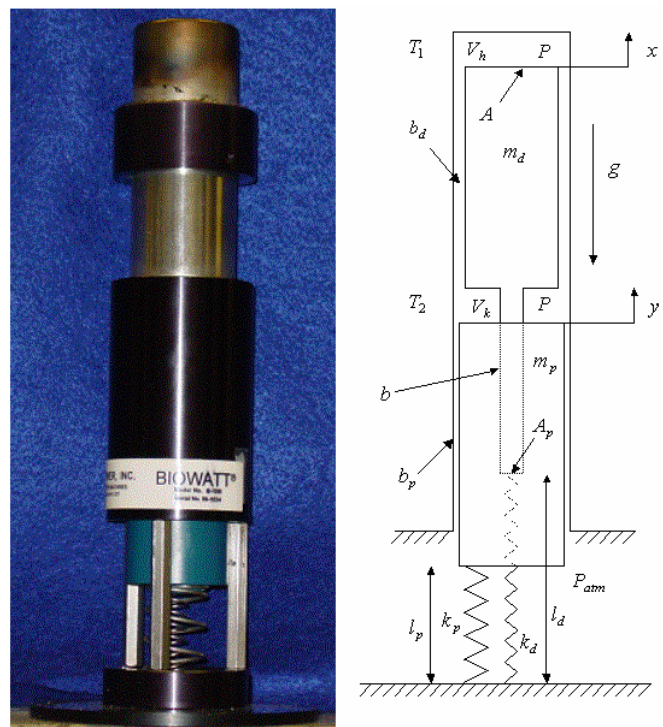
Figure 2: Picture and schematic of Sunpower B-10B free-piston Stirling demonstrator

Even though thermodynamic methods and intuitive design techniques have been vital for the development of Stirling engines, little work has been done on applying dynamic and control methods to investigate their stability and frequency characteristics. The work by Redlich and Berchowitz [4] is one of only a handful of papers that utilizes control theory concepts to analyze the linearized dynamics of such engines. Although the paper presents an analysis of free-piston Stirling engines that agree well with their experimental operation, the control concepts presented are not used to suggest a design procedure for including new combinations of either traditional or new Stirling engine elements (such as diaphragms). More generally, the literature regarding the analysis of such engines typically contains little constructive design insight. It is recognized that the design of such engines is more of an art than a constructive well-understood process [5].

This paper presents a control-based approach to "digest" the complex dynamics of Stirling engines within a design context. The operation of a free-piston stirling engine is viewed as a feedback system with a physical control law dependent on system parameters and an overall control gain related to the temperature difference across the engine. Free-piston Stirling engines are therefore viewed simply as a group of dynamic elements in a feedback configuration such that linear control techniques can be applied to optimize their performance. Standard control tools such as root locus, frequency response (Bode plots) and the Nyquist stability criterion are utilized to gain fundamental insight regarding the dynamic behavior of the system and how the variation of system parameters (through design) affects the overall dynamics. This approach will show that an *unstable* oscillatory response is desired in a linear sense in order to produce power in the true device. Unique notions such as "instability margins" and "instability robustness" will be presented and examined. Additionally, with this approach, it is shown that matching the power output of the device with any given load, such as a hydraulic or pneumatic pump or an electrical alternator, becomes a trivial matter which is subsumed as simply including more dynamics in the loop. With proper tuning and scaling, it is envisioned that such free-piston Stirling engines will have much higher power densities and be well suited as portable power supplies for applications such as untethered robotic devices.

II. METHODOLOGY

For the scope of this paper, the proposed methodology is to develop a dynamic model of the free-piston Stirling engine shown in Figure 2, and offer a control-based characterization of it. An experimental run of the device will be compared to the characteristics predicted by the linear control systems analysis.

The equations of motion of the system shown in Figure 2 are given by:

$$m_d \ddot{x} = -PA + P(A - A_r) + P_{atm} A_r - k_d (x - l_d) \\ - b_d \dot{x} - b(\dot{x} - \dot{y}) - m_d g \tag{1}$$

$$m_p \ddot{y} = -P(A - A_r) + P_{atm} A_r - k_p (y - l_p) \\ - b_p \dot{y} - b(\dot{y} - \dot{x}) - m_p g \tag{2}$$

Considering $x = 0$ and $y = 0$ to be at the point of vertical static equilibrium (when the engine is not yet running), the following relationships can be derived from Equations (1) and (2):

$$k_d l_d = m_d g + P_0 A_r - P_{atm} A_r \tag{3}$$

$$k_p l_p = m_p g + P_0 (A - A_r) - P_{atm} (A - A_r) \tag{4}$$

Equations (3) and (4) show the equilibrium lengths of the springs due to gravity and the pressure difference across the elements. This pressure difference exists if the engine is pre-pressurized prior to operation.

Adding zero to Equation (1) in the form of $+P_0 A_r - P_0 A_r$, and substituting $k_d l_d$ by Equation (3), the following expression is obtained:

$$m_d \ddot{x} = -(P - P_0) A_r - k_d x - b_d \dot{x} - b(\dot{x} - \dot{y}) \tag{5}$$

Similarly, adding $+P_0(A - A_r) - P_0(A - A_r)$ to Equation (2) and substituting $k_p l_p$ by Equation (4), we obtain:

$$m_p \ddot{y} = -(P - P_0)(A - A_r) - k_p y - b_p \dot{y} - b(\dot{y} - \dot{x}) \tag{6}$$

The next step is to incorporate the pressure dynamics into the model. The pressure in the working space fluctuates as the displacer shifts the working gas back and forth between the heater and cooler spaces. This fluctuation is given by the following commonly accepted isothermal model by Schmidt [6]:

$$\hat{P} = mR \left[\frac{V_c}{T_k} + \frac{V_k}{T_k} + \frac{V_r \ln(T_h/T_k)}{(T_h - T_k)} + \frac{V_h}{T_h} + \frac{V_e}{T_h} \right]^{-1} \tag{7}$$

For the device considered, V_c, V_r and V_e are small compared to V_k and V_h, and Equation (7) can therefore be simplified as:

$$\hat{P} = mR \left(\frac{V_k}{T_k} + \frac{V_h}{T_h} \right)^{-1} \tag{8}$$

In order to utilize this non-linear relationship within the context of linear control analysis applied to a system of linear dynamic equations, it must first be linearized. For convenience, this is done about the initial volumes V_{k0} and V_{h0}, which coincide with positions $x = 0$ and $y = 0$. The linearization is as follows:

$$P \approx P_0 + \left. \frac{\partial \hat{P}}{\partial V_h} \right|_{\substack{V_k = V_{k0} \\ V_h = V_{h0}}} (V_h - V_{h0}) + \left. \frac{\partial \hat{P}}{\partial V_k} \right|_{\substack{V_k = V_{k0} \\ V_h = V_{h0}}} (V_k - V_{k0}) \tag{9}$$

Additionally, as can be seen from Figure 2, the volumes V_h and V_k are linked to x and y by the following relationships:

$$V_h = V_{h0} - Ax \qquad (10)$$

$$V_k = V_{k0} + (A - A_r)x - (A - A_r)y \qquad (11)$$

Evaluating the partial derivatives in Equation (9), and combining these with Equations (10) and (11), the following expression is obtained,

$$P - P_0 = (C_1 A - C_2 A + C_2 A_r)x + C_2(A - A_r)y \qquad (12)$$

where C_1 and C_2 are constants given by:

$$C_{(1,2)} = mR\left(\frac{V_{h0}}{T_1} + \frac{V_{k0}}{T_2}\right)^{-2}\left(\frac{1}{T_{(1,2)}}\right) \qquad (13)$$

It is important to note that Equation (12) constitutes an input term to the coupled system dynamics of Equations (5) and (6). Further, this "input term" is a function of the states of the system. This interpretation will serve to cast the problem as a standard feedback control.

Now that we have the linearized system equations (5), (6), and (12), they can be represented in the Laplace domain as:

$$\left[m_d s^2 + (b + b_d)s + k_d\right]X = -(P - P_0)A_r + bsY \qquad (14)$$

$$\left[m_p s^2 + (b + b_p)s + k_p\right]Y = -(P - P_0)(A - A_r) + bsX \qquad (15)$$

$$(P - P_0) = (C_1 A - C_2 A + C_2 A_r)X + C_2(A - A_r)Y \qquad (16)$$
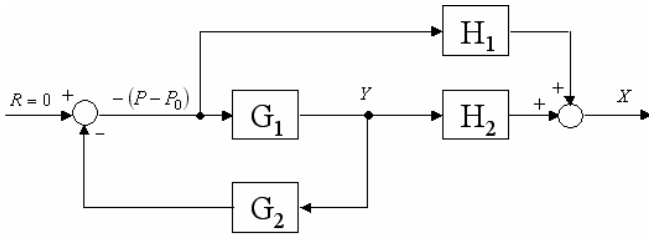
Figure 3: Block Diagram of Linearized System

Figure 3 shows the feedback block diagram obtained from the system equations. The physical-feedback loop containing the transfer functions G_1 and G_2 completely characterizes the stability and frequency response of the system. Transfer functions H_1 and G_2 are causal feed-forward filters, and do not affect the closed-loop behavior of the system. The derivation of these causal transfer functions, $\frac{Y(s)}{-(P-P_0)} = G_1(s)$, $\frac{(P-P_0)}{Y(s)} = G_2(s)$, and $X(s) = -(P-P_0)H_1(s) + Y(s)H_2(s)$ from Equations (14), (15) and (16) is algebraically simple. However, due to their large size, they are not explicitly shown in this paper. Since G_1 and G_2 can be expressed as the ratios of polynomials of s, N_1/D_1 and N_2/D_2, respectively, the closed-loop characteristic equation becomes

$$1 + \frac{N_1 N_2}{D_1 D_2} = 1 + kG_3 = 0 \qquad (17)$$

where k is a constant (or a group of constants) algebraically pulled out from $G_1 G_2$, and can be considered a controller gain whose variance marks the trajectories of the root locus.

The value of k is important, since it contains important design parameters, and allows us to see the direct effect of the system parameters on the closed-loop dynamics.

III. CONTROL TOOLS

In order to assess Equation (17) analytically via the standard root locus technique, it is necessary that the parameters contained in k are not present anywhere in G_3. In our case, we are particularly interested in looking at the trajectories as T_h (the temperature in the hot side) varies, as well as b (the coefficient of viscous friction between the displacer and the piston) and b_p (the coefficient of viscous friction between the piston and the cylinder wall). These last two are particularly important because they are closely related to the power output of the device (if, for instance, coupled with a linear alternator). Because of the high complexity of this system, the parameters in question are deeply embedded in G_3 and/or do not appear linearly, and cannot be analytically factored out as a constant k. Instead, a computational algorithm iteratively calculates the closed-loop poles as the desired parameter varies within a reasonable range, and these are plotted to generate the locus.

For the scope of this paper, the parameters used in all the calculations were measured from the Sunpower B-10B Stirling demonstrator (Figure 2). Some of the most important values to indicate are:

$$A = 10\,\text{cm}^2 \qquad A_r = 1.58\,\text{cm}^2 \qquad b = 10\,\frac{\text{N}\cdot\text{s}}{\text{m}}$$

$$b_p = 0.1\,\frac{\text{N}\cdot\text{s}}{\text{m}} \qquad m_d = 75\,\text{g} \qquad m_p = 465\,\text{g}$$

Figure 4 shows the root locus of the system as T_h increases. The square boxes indicate the position of the closed-loop poles under normal operating conditions. The normal operating value of T_h is about 600 K, and T_k is assumed to remain at room temperature. From Figure 4, it should be noted that the open-loop poles (where the trajectories originate for a theoretical value of $T_h = 0$) are all in the left-hand plane. As T_h increases past 360 K, a complex conjugate pair of closed-loop poles cross into the right-half-plane. For larger values of T_h, it can be seen that these poles increase in frequency and remain in the right-hand plane, which is desired. This agrees with the premise that from a controls perspective, a Stirling engine needs to remain unstable in order to operate. It should be emphasized that "unstable" in a linear sense represents an unbounded system energy that will represent power production in an actual physically bounded device.

Similarly, we can examine the effect of the closed-loop pole locations visualized on the root locus as the viscous friction is varied. Since the effect of b and b_p on the locus are very similar, only one is shown here. Figure 5 shows the
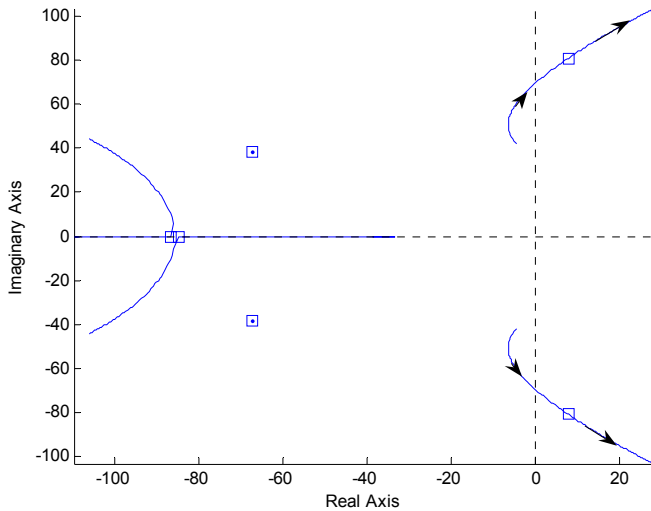
Figure 4: Root Locus Trajectories for Varying Values of T_h

root locus as b_p increases. For low enough values of this friction, the system is unstable and will operate desirably to produce net output power. However, as b_p increases, the locus trajectories will eventually cross the imaginary axis and the system will stabilize and cease to work properly (cease to produce power).
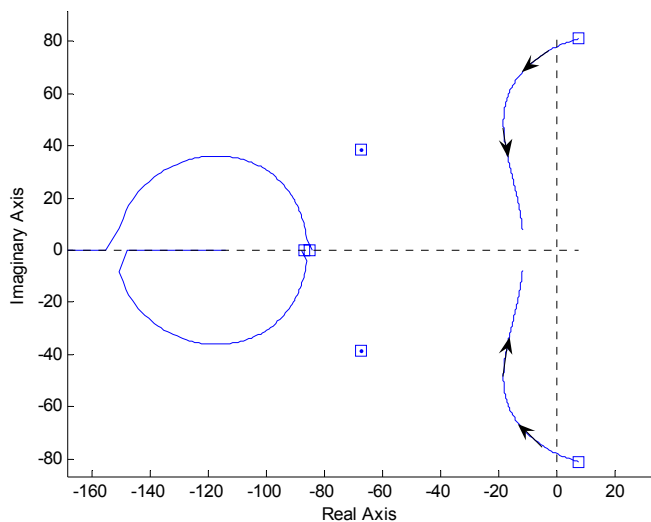
Figure 5: Root Locus Trajectories For Varying Values of b_p

It should be noted that the closed-loop pole locations for the parameter values measured and for $T_h = 600\,\mathrm{K}$ are the same in both Figures 4 and 5. The magnitude of the imaginary component of the unstable poles indicates that the linear device operates with a frequency of 12.87 Hz. This very closely matches the experimentally measured frequency of 12.82 Hz. From a design perspective, this close match highlights the adequacy of applying linear control tools for the frequency analysis of free-piston Stirling engines. Maximizing this frequency while minimizing the moving

piston and displacer masses is key for increasing the power density. However, down-scaling these devices has proven problematic given that losses such as viscous friction in the piston seals and leakage (blow-by) dominate at small scales. Since graphic control tools free us from an intuitive pictorial depiction of how these engines operate, it allows for a more fundamental design perspective, perhaps steering away from traditional sliding piston devices.

Examining the Bode and Nyquist plots we can confirm the *instability* of the system, and examine the gain and phase margins that ensure this instability. Figure 6 shows the Bode plots of the open-loop system. It shows a *negative* gain margin of 15.88 and a *negative* phase margin of 17 degrees. Even though the phase plot crosses the '−180' line twice, it is evident that the gain margin is given by the first crossing, since it's the only negative of the two. This will be verified in the Nyquist plot.
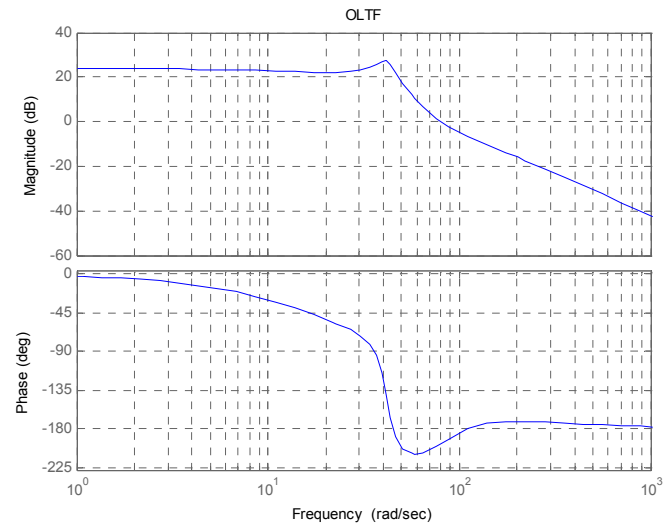
Figure 6: Open-Loop Bode Plots

The Nyquist plot of the system is shown in figure 7. Since the number of open-loop poles is zero, and there are two clock-wise encirclements about the $-1 + 0\mathrm{j}$ point, the Nyquist stability criterion confirms that there should be two unstable closed-loop poles. A unit circle was drawn around the origin in order to examine the gain and phase margins. Starting with the phase margin, the intersections between the trajectories and the unit circle occur at ±17 degrees from the negative real axis. Since our system is unstable, we know the correct phase margin is the negative one. Similarly, the gain margin for an *unstable* system is determined by the real axis crossing outside the unit circle, which in this case happens at -15.88 dB. These values are in agreement with the Bode plots and root locus stability analysis. The concept of negative gain and phase margins, or 'instability' margins, though unusual, are simply the amount of gain or phase needed to make the system stable. The *negative* gain margin implies that a reduction of the overall gain of the system is needed to achieve stability. The *negative* phase margin

indicates the amount by which the phase would need to be reduced to achieve stability. In this sense, these margins indicate how robust the instability is.
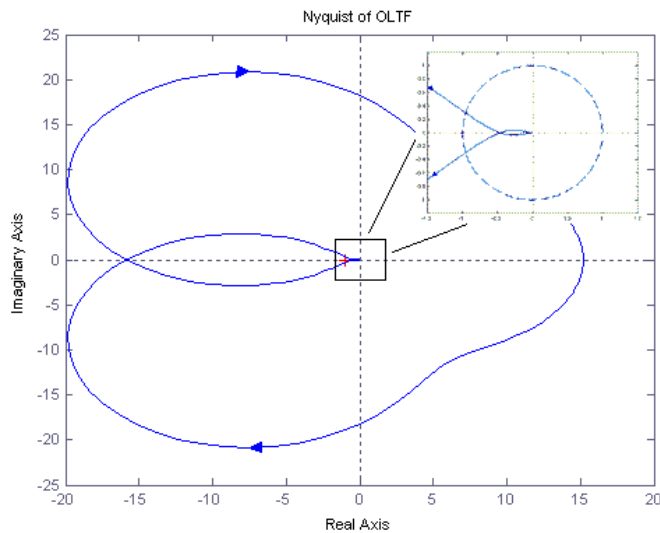
Figure 7: Open-Loop Nyquist Plot.

IV. DISCUSSION

Even though free-piston Stirling engines have been heavily studied over the past 40 years, the academic literature contains very little work on dynamics and control approaches to their study or design. The aim of this paper is to show that a simple linear control-based analysis can provide insightful information regarding fundamental operational characteristics of these engines, which could otherwise not be trivially obtained with typical thermodynamic approaches. The idea of designing for instability is also unusual, but it is shown that the control tools can be applied in the same way as in the standard case of stability design, to the extent of examining atypical notions such as *instability margins*, and *instability robustness*. Additionally, this approach allows a free-piston Stirling design to not rely so much on intuitive notions and fine tuning, but instead on a systems' level understanding as a whole. The linear control techniques shown here should suffice in determining whether or not the system parameters are adequate enough for it to run properly, and they can also serve as a strong troubleshooting tool.

Another important objective of this analysis was to show that free-piston Stirling engines can be viewed as a conglomerate of interacting dynamic elements, which can allow for some outside-the-box thinking. Regardless of the order or complexity of the system, these simple control tools can be used to 'digest' all the complicated dynamics in the system, and focus only on the dominant poles, which contain all the information regarding instability and frequency response.

In the linear sense, for a free-piston Stirling engine to be unstable means that its output power grows unbounded, by means of ever-increasing closed-loop physical feedback. In a real nonlinear device, however, this power is harnessed either purposefully or absorbed through collisions, and the shape of the response is bounded. Techniques for maximizing the power output and power transfer to a load are outside the scope of this paper, but well within the motivation and intent for future work. In actual design, impedance matching and application of the maximum power transfer theorem should be considered, as well as optimizing the power density of the device. As noted in the introduction, one of the largest shortcomings of Stirling technology to date has been its limited power density.

The authors envision that small-scale free-piston Stirling devices, given their outstanding theoretical energy and power densities, simplicity, quietness, and fuel flexibility pose as excellent candidates for portable power suppliers for untethered human-scale machines. In the framework of the analysis presented here, the load coupled to such device would present itself as merely an added dynamic element (or elements), such that operational optimization can be achieved in a similar way regardless of the nature of the load.

V. CONCLUSIONS

A control-based design approach of free-piston Stirling engines was presented, and introduced as potential small scale ($\leq 1\,\text{kW}$) portable power supply for untethered robots. The motivation is based on the current limitations of sources of power, such as batteries, as well as the growing search for alternative sources of energy. The approach taken is unusual in the sense that Stirling engines need to be in an unstable mode in order to run properly; the control techniques are applied in such a way that a robustly unstable oscillatory response is maintained. It was shown that these tools apply to instability control in a very similar way as with stability control, and standard concepts and tools such as root locus analysis, gain and phase margin and the Nyquist stability criterion are just as useful in designing a robustly unstable system as they are in designing a robustly stable system.

REFERENCES

[1] Goldfarb, M., Barth, E. J., Gogola, M. A., Wehrmeyer, J. A., "Design and Energetic Characterization of a Liquid-Propellant-Powered Actuator for Self-Powered Robots". *IEEE/ASME Transactions on Mechatronics*, vol. 8, no. 2, pp. 254-262, June 2003.

[2] Walker, G., and J. R. Senft, *Free Piston Stirling Engines*, Berlin: Springer-Verlag, 1985.

[3] Urieli, Israel, and David M. Berchowitz, *Stirling Cycle Engine Analysis*, Bristol: Adam Hilger Ltd, 1984.

[4] Redlich, R. W. and Berchowitz, D. M. "Linear Dynamics of Free-Piston Stirling Engines," *ImechE*, pp. 203-213, 1985.

[5] Beale, W.T. "The Free Piston Stirling Engine: 20 Years of Development," *IECEC*, pp. 689-693, 1983.

[6] Schmidt, G. "The Theory of Lehmann's Calorimetric Machine," *Z. Ver. Dtsch. Ing*, vol. 15, part 1.